A Dual-Band Ring-Resonator Bandpass Filter Based on Two Pairs of Degenerate Modes

Sha Luo, *Student Member, IEEE*, Lei Zhu, *Senior Member, IEEE*, and Sheng Sun, *Member, IEEE*

***Abstract*—In this paper, a class of dual-band ring-resonator bandpass filters is proposed based on a single ring resonator. As its most distinctive feature, two pairs of first- and second-order degenerate resonant modes in a ring resonator are simultaneously excited, resulting in a compact dual-mode dual-band bandpass filter with two transmission poles in both passbands. Firstly, two capacitors or parallel-coupled lines are placed at two nonorthogonally excited positions along a ring resonator in order to excite the two first-order degenerate modes and create multiple transmission zeros. Next, a set of perturbations is introduced on the ring to excite the two second-order degenerate modes. In our design, two excitation positions are first placed with between 45°- and 135°-separation on a ring. Simulations show that, with a proper arrangement of the excitation angle, two transmission poles in the first passband can be excited and more transmission zeros can be generated. Four and eight open-circuited stubs are loaded symmetrically along the ring, resulting in synchronous excitation of two poles in the second passband. Of the two designed filters with 135°- and 45°-separation, the one with 45° exhibits much better out-of-band performance with three additional transmission zeros at frequencies lower than the first passband, between the two passbands and higher than the second passband. Finally, two filter prototypes are fabricated and their measured results are found to be in good agreement with theory.**

***Index Terms*—Bandpass filter, dual band, dual mode, open-circuited stubs, ring resonator, transmission zeros.**

I. Introduction

MICROSTRIP ring resonators have been intensively studied and used in various microwave circuits such as antennas, bandpass filters, couplers, oscillators, and mixers [1]. It is well understood that there are two degenerate orthogonal modes, TM_{10} and TM_{01}, coexisting in a symmetric ring resonator. In order to split these two degenerate modes, the internal coupling between the two resonant modes needs to be created by either changing the angle between the excitation ports or adding perturbations in a plane orthogonal to the ring resonator [2]. Designing a bandpass filter using a dual-mode ring resonator has the advantages of compact size and high quality (Q) factor . A lot of research has been done to explore dual-mode ring resonator bandpass filters with a single narrow passband [3]–[13]. In [3], a small triangle patch acting as a perturbation was attached to an inner corner of the square loop to excite the pair of degenerate modes. The strength and nature of the coupling between the degenerate modes, which are determined by the size and shape of the perturbation, have been studied [4]. By varying the position of the perturbation along a hexagonal ring, the number and locations of the transmission zeros can be adjusted close to the passband [5]. A simple stepped-impedance ring resonator was proposed in [6] to control the coupling strength of the two fundamental degenerate modes. The upper stopband performance was improved by using a periodic structure, as demonstrated in [7]. Moreover, different coupling mechanisms have been discussed for a dual-mode bandpass filter implementation, e.g., line-to-ring coupling [8], enhanced side-coupling [9], meander-line embedded coupling [10], self-coupled ring resonator [11], and quarter-wavelength side-coupling [12]. In [13], the coupling between the two degenerate modes can be kept constant by adjusting both the stub perturbations and angle between the excitation ports, while the frequencies of the two transmission zeros shift in the two sides of the desired passband.

In recent years, various dual-band bandpass filters have been extensively studied and developed to meet requirements in modern multiband wireless communication systems. Of them, the dual-mode dual-band filters using ring resonators [14]–[21] have garnered a lot of attention due to their compactness. In [14], a stepped-impedance ring resonator was proposed to design a dual-band filter with adjustable first- and second-order resonant frequencies. Unfortunately, only a single transmission pole could be created in the second passband for a single ring resonator filter. Subsequently, two dissimilar ring resonators with different resonant frequencies were individually designed and properly linked together [15]–[18] to achieve the desired dual-passband performance. In these cases, the two ring resonators were vertically stacked in a two-layer substrate [15], [16], or implemented in the same layer [17], [18]. As a result, the solutions need more design considerations and larger overall size.

In [19] and [20], two compact dual-mode dual-band bandpass filters based on a single ring resonator were designed. Instead of a common two-port excitation angle, i.e., either 90° or 180°, the two excitation ports were placed at 135°-separation. In [19], the two pairs of the first- and third-order degenerate modes of the ring resonator were excited and utilized to form two passbands individually. However, two additional impedance transformers are needed in the final design and thus enlarge the overall size. Alternatively, two operating passbands can also be realized by using the two pairs of the first- and second-order degenerate modes of a ring resonator. This kind of dual-band filter was

Manuscript received February 10, 2010; revised February 10, 2010; accepted June 06, 2010. Date of publication July 19, 2010; date of current version December 10, 2010. This paper is an expanded paper from the Asia–Pacific Microwave Conference, Singapore, December 7–10, 2009.

S. Luo and L. Zhu are with the School of Electrical and Electronic Engineering, Nanyang Technological University, Singapore (e-mail: luos0002@ntu.edu.sg; ezhul@ntu.edu.sg).

S. Sun is with the Institute of Microwave Techniques, University of Ulm, Ulm 89081, Germany (e-mail: sunsheng@ieee.org).

Color versions of one or more of the figures in this paper are available online at http://ieeexplore.ieee.org.

Digital Object Identifier 10.1109/TMTT.2010.2053590

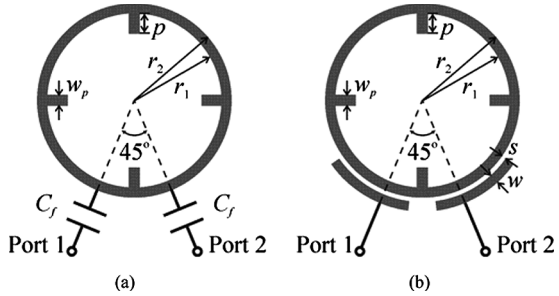

Fig. 1. Schematic of the proposed ring resonator with two distinct excited structures. (a) By lumped capacitors. (b) By parallel-coupled lines.

proposed in [20] and does not need any external matching network. However, this initial filter still suffers from a poor selectivity in a range out of the desired two passbands. A class of dual-mode dual-band ring resonator bandpass filters using microwave C-sections was recently reported in [21]. The excitation angle was selected to be 60°, but there is no detailed discussion on the design procedure of these filters including how to choose a proper excitation angle.

The motivation of this paper is to give a unified description on the operating principle and design procedure of a novel dual-mode dual-band ring-resonator bandpass filter enhancing the work in [20]. For this purpose, our first step is to characterize the relationship between the transmission zero locations and the angle between the two excitation ports along a uniform ring resonator. To achieve a sufficient number of transmission zeros and to keep a certain spacing between the two ports for installing the coupling elements, a separation of 45° is eventually selected. Fig. 1(a) and (b) shows the schematic of a microstrip ring resonator that is capacitively fed by lumped capacitors and coupled lines, respectively. Our next step is to discuss synchronous excitation of the two degenerate modes in both passbands via enhanced coupling strength at the ports and stretched perturbation stubs. Finally, the two compact dual-mode dual-band filters using a single microstrip ring resonator are designed with four and eight stubs using equivalent-circuit models and the ADS Momentum simulator [22]. Measured results of the two fabricated filter prototypes verify the proposed design principle.

II. Transmission Zeros in a Ring Resonator

Fig. 2(a) depicts the schematic of a uniform ring resonator that is excited by two identical lumped capacitors (C_f) at an arbitrary separation angle (ϕ) between two excitation ports. In its equivalent model [see Fig. 2(b)] Z_r represents the characteristic impedance of the ring, while θ_1 and θ_2 are the electrical lengths of the short and long paths of a ring between the two ports, respectively. Under very weak capacitive coupling at the ports, the resonances or transmission poles occur at

$$\theta_1 + \theta_2 = 2n \times 180^\circ, \qquad \text{for } n = 1, 2, 3 \ldots. \tag{1}$$

Due to the transversal interference between the two signal paths from one port to the other port, as discussed in [23], the resultant transmission zeros appear at

$$\theta_2 - \theta_1 = (2m+1) \times 180^\circ, \qquad \text{for } m = 0, 1, 2, \ldots. \tag{2}$$

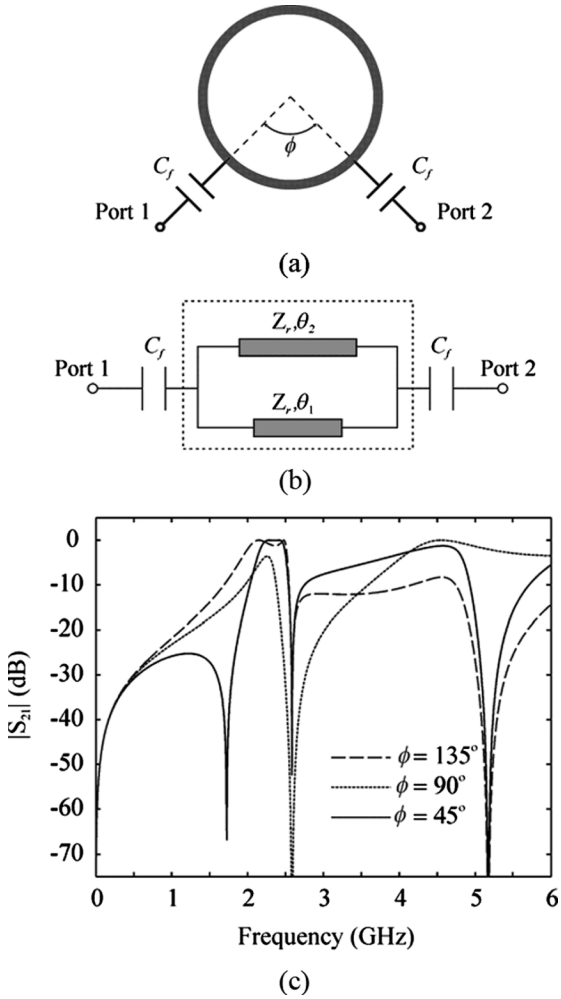

Fig. 2. (a) Schematic of a uniform ring resonator with two lumped capacitors at the excitation positions. (b) Its equivalent model. (c) Frequency responses of S_{21}-magnitudes under varied excitation angles (ϕ) with $C_f = 0.8$ pF and $Z_r = 73\ \Omega$.

It is of interest to note that the case considered in [20] is a special case of (2), where $\theta_r = \theta_2 - \theta_1$, $\theta_1 = 3\theta_r/2$, and $\theta_2 = 5\theta_r/2$.

Fig. 2(c) illustrates three sets of frequency responses of the S_{21}-magnitudes under varied excition angles. At the first resonance, the overall electrical length of this ring resonator is equal to 360°, thus enforcing $\phi = \theta_1 = 360^\circ - \theta_2$. When $\phi = 135^\circ$, $\theta_2 = 225^\circ = 5\theta_1/3$. In this situation, the first transmission zero from (2) is determined by setting $m = 0$, thus deriving $\theta_1 = 270^\circ$ and $\theta_2 = 450^\circ$, where $\theta_2 - \theta_1 = 180^\circ$. This transmission zero from the out-of-phase cancellation appears at 5.21 GHz in Fig. 2(c). As ϕ is reduced to 90°, $\theta_2 = 3\theta_1$ can be obtained. The transmission zero moves to the frequency [approximately equal to 2.65 GHz for the case in Fig. 2(c)] with $\theta_1 = 90^\circ$ and $\theta_2 = 270^\circ$, and it is exactly placed at the first resonant frequency of this ring resonator. As such, this first resonance can hardly be excited if the coupling at the ports is not sufficiently high [2]. As ϕ is further decreased to 45°, $\theta_2 = 7\theta_1$ is attained. In this case, the transmission zero occurs at 1.80 GHz [see Fig. 2(c)], where $\theta_1 = 30^\circ$ and $\theta_2 = 210^\circ$, and it is located lower than the first resonant frequency [close to 2.35 GHz shown in Fig. 2(c)] where $\theta_2 + \theta_1 = 360^\circ$. At the frequency with $\theta_1 = 90^\circ$ and $\theta_2 = 630^\circ$, the two signals traversing the

short and long paths become out of phase again, resulting in suppression of the second resonant mode. Up to now, we have discussed that multiple transmission zeros and their locations can be excited and changed via the angle between the two excitation ports along a uniform ring resonator. Of the three cases in Fig. 2(c), the last structure with $\phi = 45°$ will be used to design two dual-band bandpass filters with good out-of-band performance due to the existence of more transmission zeros including the zero at the lower stopband of the first passband.

III. Principle and Geometry of Proposed Filters

A. Ring Resonators With Lumped Capacitors

Let us go back to look at Fig. 1(a) again where a stubs-loaded ring resonator is fed at the input and output ports via lumped capacitors (C_f). In this figure, r_1 and r_2 are the inner and outer radii of this ring. The four identical open-circuited stubs are electrically attached to the ring resonator with equal spacing, width of w_p, and length of p. Fig. 3(a) is the equivalent transmission-line circuit model under the undisturbed condition, i.e., $p = 0$ mm. Based on the above discussion, the longer path with θ_2 in Fig. 2(b) is seven times the shorter path with θ_1 in electrical length, i.e., $\theta_2 = 7\theta_1$. As shown in Fig. 3(c) for the curve with $p = 0$ mm, two transmission poles visibly emerge in the first passband under the selected capacitance of $C_f = 0.8$ pF, indicating that the two first-order degenerate modes are successfully split under the selection of a 45° excitation angle. 0.8 pf is used to provide proper coupling for the dual-passband of the filter. To give physical insight into this phenomenon, the two external ports are excited under even- and odd-mode sources. Under these two distinct excitations, the symmetrical plane in Fig. 3(a) becomes the perfect magnetic wall (M.W.) and electric wall (E.W.), respectively. Its bisection becomes a one-port network with open- and short-circuited ends in the M.W. and E.W. locations accordingly. As indicated in Fig. 3(a), Y_l and $Y_r^{e,o}$ represent the two input admittances at two ports, looking into the left and right sides of this one-port bisection network. Under the even-mode excitation, all the resonant frequencies must satisfy

$$\mathrm{Im}\,(Y_l + Y_r^e) = 0 \tag{3}$$

where

$$Y_l = \frac{j\omega C_f}{1 + j\omega C_f Z_0} \tag{4}$$

$$Y_r^e = jY_r\left(\tan\frac{\theta_1}{2} + \tan\frac{7\theta_1}{2}\right) \tag{5}$$

in which ω is the angular frequency and $Y_r = 1/Z_r$. Similarly, resonances under the odd-mode excitation occur at

$$\mathrm{Im}(Y_l + Y_r^o) = 0 \tag{6}$$

where

$$Y_r^o = -jY_r\left(\cot\frac{\theta_1}{2} + \cot\frac{7\theta_1}{2}\right). \tag{7}$$

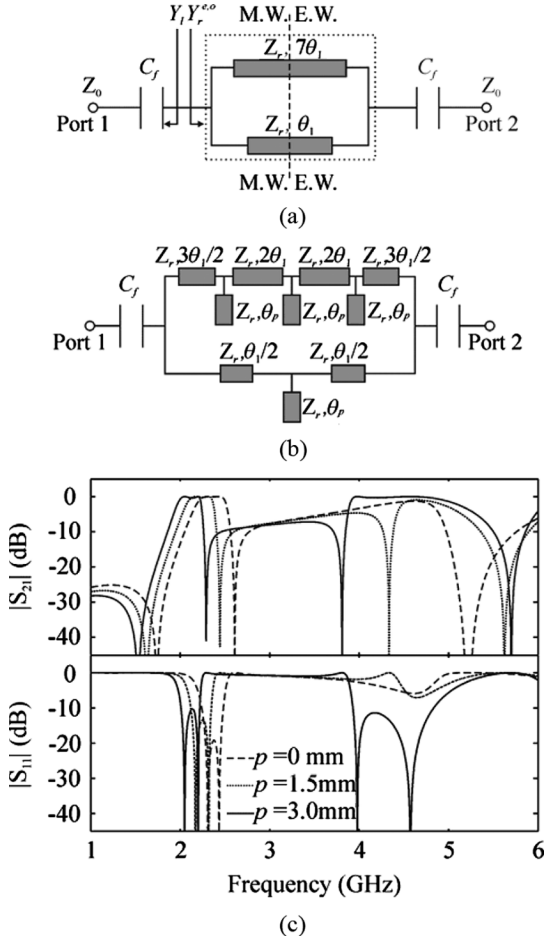

Fig. 3. (a) Equivalent model of a uniform ring resonator with a separation of 45°. (b) Equivalent model of the stub-loaded ring resonator in Fig. 1(a). (c) Frequency responses of S-magnitudes under varied stub lengths (p) ($C_f = 0.8$ pF, $Z_r = 73\ \Omega$, and $Z_0 = 50\ \Omega$).

As explained above, one transmission zero appears at the lower stopband of the first passband, while the second passband can be fully suppressed by a higher transmission zero under a weak coupling case. Regardless, all the transmission zeros always happen at the frequencies where the resultant mutual admittance (Y_{21}) of the two-port network inside the dashed square in Fig. 3(a) equals to zero, such that

$$Y_{21} = jY_r\left(\frac{1}{\sin\theta_1} + \frac{1}{\sin 7\theta_1}\right) = 0. \tag{8}$$

By solving (8), all of the transmission zeros can be determined as follows:

$$\theta_1 = \frac{2a+1}{4}\pi \qquad \text{for } a = 0, 1, 2, \ldots \tag{9}$$

$$\theta_1 = \frac{2b+1}{6}\pi, \qquad \text{for } b = 0, 1, 2, \ldots. \tag{10}$$

In particular, we can notice that (10) represents the same condition as (2) that is from the signal-interference technique. For the undisturbed case, $b = 0$ and $b = 1$ in (10) determine the first and third transmission zeros, respectively, while the second

zero at the right side of the first passband is derived with $a = 0$ in (9).

After achieving the first passband with the help of two poles, four open-circuited stubs are added symmetrically along the ring, as shown in Fig. 3(b), which act as the perturbation elements to produce the second passband with two poles. As illustrated in Fig. 3(c), as p increases from 1.5 to 3.0 mm, the second passband is stimulated with one or two poles. In the meantime, two transmission zeros are observed at both sides of the second passband. These zeros are created by the same nature of perturbation for a classical dual-mode filter, as discussed in [4].

B. Ring Resonators With Parallel-Coupled Lines

Fig. 1(b) displays a fully integrated ring resonator fed by two identical parallel-coupled lines with a spacing of s and width of w or $r_2 - r_1$. Following the analysis of a pair of three-port coupled lines in [24], the equivalent-circuit model of a three-port network using parallel-coupled lines is obtained as shown in Fig. 4(a) and it has the effective electrical lengths of θ_3 and θ_4 for the lower and upper coupling sections, respectively. For the parallel-coupled lines, their even- and odd-mode characteristic impedances are given as Z_{0e} and Z_{0o}, respectively. Under the equivalence of the two networks in Fig. 4(a), the capacitance in the right-side network can be found for our design application, and its capacitive impedance Z_c can be expressed as

$$Z_c = -2j\frac{Z_{0e}Z_{0o}}{(\tan\theta_3 + \tan\theta_4)(Z_{0e} + Z_{0o})}. \tag{11}$$

The turns ratio of voltage transformer, N, and characteristic impedance of equivalent transmission lines at port 2 and 3, Z, were obtained in our earlier wok [19], and they are given as

$$N = \frac{Z_{0e} + Z_{0o}}{Z_{0e} - Z_{0o}} \tag{12}$$

$$Z = \frac{Z_{0e} + Z_{0o}}{2}. \tag{13}$$

Fig. 4(b) shows the complete equivalent-circuit model for the proposed ring-resonator filter in Fig. 1(b). Fig. 4(c) illustrates the three sets of simulated results. It can be used to reveal the design principle and procedure again for the fully integrated filter in Fig. 1(b) under the consideration herein. For $p = 0$ mm, the two first-order degenerate modes are split due to the tight coupling of the coupled lines placed at two nonorthogonal excitation ports at a frequency close to $f_0 = 2.4$ GHz (fundamental resonant frequency of the uncoupled ring resonator). As p is increased to 0.5 mm, the S_{21}-magnitudes move up at around 5.0 GHz and thus form the second passband with a single transmission pole. As p is further lengthened to 1.0 mm, the two second-order degenerate modes are split and thus make up the second passband with two visible transmission poles. As can be observed in Fig. 4(c), the four attached stubs cause a slight lowering of the first passband, but they do not significantly influence the filtering configuration in this first passband. To this end, the proposed ring-resonator bandpass filter in Figs. 1(b) and 4(b) has been verified to show two passbands and two transmission poles in each passband. Based on the above discussion, it can be understood that the filtering performance in the first passband is mainly determined by the external coupling strength of

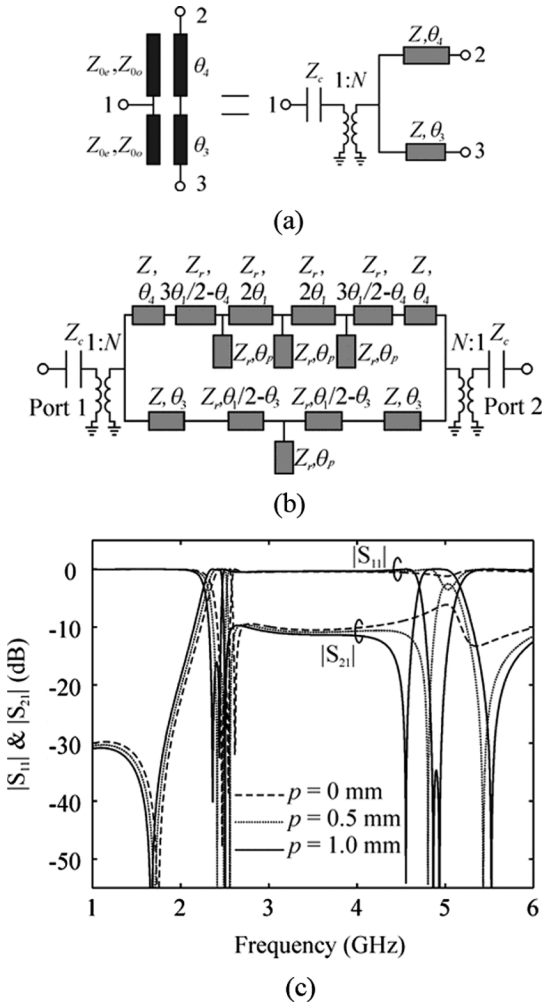

Fig. 4. (a) Schematic and equivalent model of the coupled-line structure. (b) Schematic of the ring-resonator filter with four equally spaced perturbation stubs. (c) Frequency responses of the microstrip-line filter in Fig. 1(b) under varied stub lengths (p) ($r_1 = 6.93$ mm, $r_2 = 7.33$ mm, $w_p = 0.40$ mm, $s = 0.10$ mm, $\theta_3 = \theta_1/3$, and $\theta_4 = 13\theta_1/18$. Substrate: $\epsilon_r = 10.8$, thickness $= 1.27$ mm).

the parallel-coupled lines, which are placed at two nonorthogonal positions of the ring resonator. Meanwhile, the filtering performance in the second passband is primarily dependent on the length/width of the four identical open-circuited stubs that are attached to the ring with equal spacing. In particular, under the choice of a 45°-separation, the two sets of dual transmission zeros simultaneously emerge at the lower and upper sides of each passband.

IV. Results and Discussion

Based on the analysis and initial design, the proposed compact dual-mode dual-band bandpass filter is then optimally designed using a full-wave electromagnetic (EM) simulator [22] and fabricated on a dielectric substrate with a thickness of 1.27 mm and permittivity of 10.8. Fig. 5(a) shows the photograph of the fabricated filter circuit. Fig. 5(b) plots the measured results with the circuit and EM simulated results, and it shows good agreement between them over a wide frequency range from 1.0 to 6.0 GHz. The measured center frequencies of the

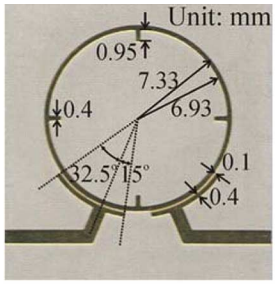

(a)

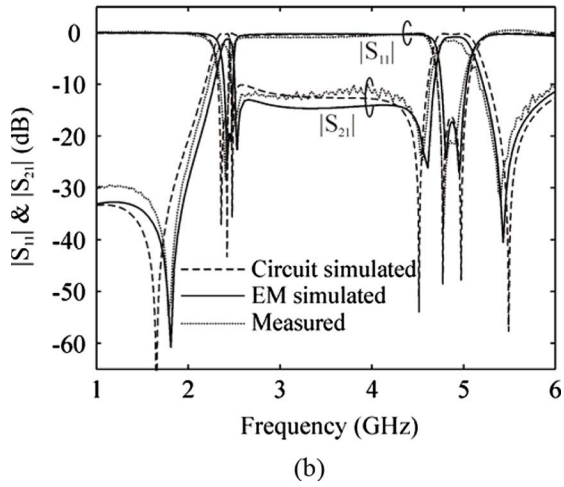

(b)

Fig. 5. (a) Photograph of the fabricated filter with four attached stubs. (b) Simulated and measured results with the stub length of $p = 0.95$ mm.

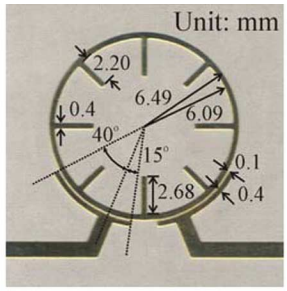

(a)

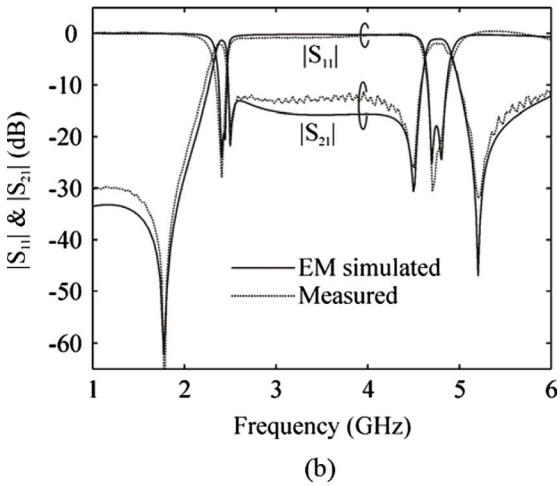

(b)

Fig. 6. (a) Photograph of the fabricated filter with four attached stubs. (b) Simulated and measured results with the stub lengths of $p = 2.20$ and 2.68 mm.

two passbands are 2.38 and 4.87 GHz, respectively. The fractional bandwidths of the two passbands are found to be 6.7% and 8.0%, respectively. The measured minimum insertion loss is around 2.0 dB in the first passband and is around 1.4 dB in the second passband. From Fig. 5(b), the four measured transmission zeros are observed at 1.79, 2.51, 4.54, and 5.39 GHz, as predicted in the analysis and simulation. With the existence of these four transmission zeros, the proposed dual-band filter achieves good filtering selectivity for both realized passbands. In particular, the measured attenuation is higher than 30.0 dB from dc to 1.93 GHz and the attenuation in a range from 2.47 to 4.63 GHz between the two passbands is higher than 11.0 dB.

To further miniaturize the overall circuit size, an alternative ring resonator is formed by adding four additional open-circuited stubs. As shown in Fig. 6(a), eight stubs have been employed here and allocated symmetrically along the ring in order to allow for sufficient spacing between them. Based on the same procedure as discussed above, a size-reduced dual-band ring-resonator bandpass filter can be formed and designed. Fig. 6(a) shows a photograph of the fabricated filter with its dimensions indicated. With the help of eight perturbation stubs, the overall physical area of the ring resonator is reduced by 22% due to the increased slow-wave factor. The EM simulated and measured results are plotted in Fig. 6(b), showing the expected dual-mode dual-band filtering performance. In addition, the measured filter operates at 2.38 and 4.77 GHz with a minimum insertion loss of 2.0 dB in both passbands. The four transmission zeros are still observable and they appear at 1.78, 2.41, 4.5, and 5.21 GHz, respectively. The measured attenuation in a range from 2.48 to 4.57 GHz between the two operating passbands is higher than 12.0 dB.

V. Conclusion

In this paper, a novel class of dual-mode dual-band bandpass filters on a single microstrip ring resonator has been presented. By using the out-of-phase cancellation of two signals along the shorter and longer paths of a ring resonator under nonorthogonal excitation, multiple transmission zeros are produced at different frequencies. As a 45°-separation between the excitation ports is chosen, a dual-band ring-resonator filter is designed to achieve the two sets of transmission zeros at the lower and higher sides of each passband. After the detailed description of the operating principle and design procedure, two compact dual-band bandpass filters have been successfully developed. The measured results have verified good dual-passband performance with good filtering selectivity for the proposed single-ring-resonator dual-mode dual-band bandpass filter topologies.

References

[1] K. Chang and L. H. Hsieh, *Microstrip Ring Circuits and Related Structures*. New York: Wiley, 2004.

[2] I. Wolff, "Microstrip bandpass filter using degenerate modes of a microstrip ring resonator," *Electron. Lett.*, vol. 8, no. 12, pp. 302–303, Jun. 1972.

[3] J. S. Hong and M. J. Lancaster, "Bandpass characteristics of new dual-mode microstrip square loop resonators," *Electron. Lett.*, vol. 31, no. 11, pp. 891–892, May 1995.

[4] A. Gorur, "Description of coupling between degenerate modes of a dual-mode microstrip loop resonator using a novel perturbation arrangement and its dual-mode bandpass filter applications," *IEEE Trans. Microw. Theory Tech.*, vol. 52, no. 2, pp. 671–677, Feb. 2004.

[5] R.-J. Mao and X.-H. Tang, "Novel dual-mode bandpass filters using hexagonal loop resonator," *IEEE Trans. Microw. Theory Tech.*, vol. 54, no. 9, pp. 3526–3533, Sep. 2006.
[6] M. Matsuo, H. Yabuki, and M. Makimoto, "Dual-mode stepped-impedance ring resonator for bandpass filter applications," *IEEE Trans. Microw. Theory Tech.*, vol. 49, no. 7, pp. 1235–1240, Jul. 2001.
[7] J.-T. Kuo and C.-Y. Tsai, "Periodic stepped-impedance ring resonator (PSIRR) bandpass filter with a miniaturized area and desirable upper stipband charateristics," *IEEE Trans. Microw. Theory Tech.*, vol. 54, no. 3, pp. 1107–1112, Mar. 2006.
[8] L. Zhu and K. Wu, "A joint field/circuit model of line-to-ring coupling structures and its application to the design of microstrip dual-mode filters and ring resonator circuits," *IEEE Trans. Microw. Theory Tech.*, vol. 47, no. 10, pp. 1938–1948, Oct. 1999.
[9] L.-H. Hsieh and K. Chang, "Dual-mode quasi-elliptic-function bandpass filters using ring resonators with enhanced-coupling tuning stubs," *IEEE Trans. Microw. Theory Tech.*, vol. 50, no. 5, pp. 1340–1345, May 2002.
[10] J. S. Hong and M. J. Lancaster, "Microstrip bandpass filter using degenerate modes of a novel meander loop resonator," *IEEE Microw. Guided Wave Lett.*, vol. 5, no. 11, pp. 371–372, Nov. 1995.
[11] Y.-H. Jeng, S.-F. R. Chang, Y.-M. Chen, and Y.-J. Huang, "A novel self-coupled dual-mode ring resonator and its applications to bandpass filters," *IEEE Trans. Microw. Theory Tech.*, vol. 47, no. 10, pp. 1938–1948, Oct. 1999.
[12] M. K. M. Salleh, G. Prigent, O. Pigaglio, and R. Crampagne, "Quarter-wavelength side-coupled ring resonator for bandpass filters," *IEEE Trans. Microw. Theory Tech.*, vol. 56, no. 1, pp. 156–162, Jan. 2008.
[13] A. C. Kundu and I. Awai, "Control of attenuation pole frequency of a dual-mode microstrip ring resonator bandpass filter," *IEEE Trans. Microw. Theory Tech.*, vol. 49, no. 6, pp. 1113–1117, Jun. 2001.
[14] T.-H. Huang, H.-J. Chen, C.-S. Chang, L.-S. Chen, Y.-H. Wang, and M.-P. Houng, "A novel compact ring dual-mode filter with adjustable second-passband for dual-band applications," *IEEE Microw. Wireless Compon. Lett*, vol. 16, no. 6, pp. 360–362, Jun. 2006.
[15] J.-X. Chen, T. Y. Yum, J.-L. Li, and Q. Xue, "Dual-mode dual-band bandpass filter using stacked-loop structure," *IEEE Microw. Wireless Compon. Lett*, vol. 16, no. 9, pp. 502–504, Sep. 2006.
[16] E. E. Djoumessi and K. Wu, "Multilayer dual-mode dual-bandpass filter," *IEEE Microw. Wireless Compon. Lett*, vol. 19, no. 1, pp. 21–23, Jan. 2009.
[17] X. Y. Zhang and Q. Xue, "Novel dual-mode dual-band filters using coplanar-waveguide-fed ring resonators," *IEEE Trans. Microw. Theory Tech.*, vol. 55, no. 10, pp. 2183–2190, Oct. 2007.
[18] A. Gorur and C. Karpuz, "Compact dual-band bandpass filters using dual-mode resonators," in *IEEE MTT-S Int. Microw. Symp. Dig.*, Jun. 2007, pp. 905–908.
[19] S. Luo and L. Zhu, "A novel dual-mode dual-band bandpass filter based on a single ring resonator," *IEEE Microw. Wireless Compon. Lett*, vol. 19, no. 8, pp. 497–499, Aug. 2009.
[20] S. Luo, L. Zhu, and S. Sun, "A dual-mode dual-band bandpass filter using a single ring resonator," in *Proc. Asia–Pacific Microw. Conf.*, 2009, pp. 921–924.
[21] Y.-C. Chiou, C.-Y. Wu, and J.-T. Kuo, "New miniaturized dual-mode dual-band ring resonator bandpass filter with microwave C-sections," *IEEE Microw. Wireless Compon. Lett*, vol. 20, no. 2, pp. 67–69, Feb. 2010.
[22] Advanced Design System (ADS). ver. 2006a, Agilent Technol., Palo Alto, CA, 2006.
[23] R. Gomez-Garcia and J. I. Alonso, "Design of sharp-rejection and low-loss wide-band planar filters using signal-interference techniques," *IEEE Microw. Wireless Compon. Lett*, vol. 15, no. 8, pp. 530–532, Aug. 2005.
[24] Y. Nemoto, K. Kobayashi, and R. Sato, "Graphy transformations of nonuniform coupled transmission line networks and their application," *IEEE Trans. Microw. Theory Tech.*, vol. MTT-33, no. 11, pp. 1257–1263, Nov. 1985.

Sha Luo (S'08) was born in Hunan Province, China. She received the B. Eng. degree from Nanyang Technological University (NTU), Singapore, in 2006, and is currently working toward the Ph.D. degree in electrical and electronic engineering at NTU.

From 2006 to 2007, she was a Research Engineer with the Satellite Engineering Communication Laboratory, Singapore. Her research interests include multilayer planar circuits, microwave filters, and millimeter-wave passive components.

Ms. Luo was the recipient of the Ministry of Education Scholarship (2002–2006), Singapore, and an NTU Research Scholarship (2007–2010).

Lei Zhu (S'91–M'93–SM'00) received the B. Eng. and M. Eng. degrees in radio engineering from the Nanjing Institute of Technology (now Southeast University), Nanjing, China, in 1985 and 1988, respectively, and the Ph.D. Eng. degree in electronic engineering from the University of Electro-Communications, Tokyo, Japan, in 1993.

From 1993 to 1996, he was a Research Engineer with the Matsushita-Kotobuki Electronics Industries Ltd., Tokyo, Japan. From 1996 to 2000, he was a Research Fellow with the Ecole Polytechnique de Montreal, University of Montreal, Montreal, QC, Canada. Since July 2000, he has been an Associate Professor with the School of Electrical and Electronic Engineering, Nanyang Technological University, Singapore. He has authored or coauthored over 190 papers in peer-reviewed journals and conferences, including 18 in the IEEE TRANSACTIONS ON MICROWAVE THEORY AND TECHNIQUES, and 32 in the IEEE MICROWAVE AND WIRELESS COMPONENTS LETTERS. His papers have been cited over 1600 times by others with the H-index of 22 (source: ISI Web of Science). He was an Associate Editor for the *IEICE Transactions on Electronics* (2003–2005). His research interests include planar filters, planar periodic structures, planar antennas, numerical EM modeling, and deembedding techniques.

Dr. Zhu has been an associate editor for the IEEE MICROWAVE AND WIRELESS COMPONENTS LETTERS since October 2006, and an associate editor for the IEEE TRANSACTIONS ON MICROWAVE THEORY AND TECHNIQUES since June 2010. He has been a member of the IEEE Microwave Theory and Techniques Society (IEEE MTT-S) Technical Committee 1 on Computer-Aided Design since June 2006. He was a general chair of the 2008 IEEE MTT-S International Microwave Workshop Series (IMWS'08) on Art of Miniaturizing RF and Microwave Passive Components, Chengdu, China, and a Technical Program Committee (TPC) chair of the 2009 Asia–Pacific Microwave Conference (APMC'09), Singapore. He was the recipient of the 1997 Asia–Pacific Microwave Prize Award, the 1996 Silver Award of Excellent Invention from the Matsushita–Kotobuki Electronics Industries Ltd., and the 1993 First-Order Achievement Award in Science and Technology from the National Education Committee, China.

Sheng Sun (S'02–M'07) received the B.Eng. degree in information and communication engineering from Xi'an Jiaotong University, Xi'an, China, in 2001, and the Ph.D. degree in electrical and electronic engineering from Nanyang Technological University (NTU), Singapore, in 2006.

From 2005 to 2006, he was with the Institute of Microelectronics, Singapore. From 2006 to 2008, he was with the School of Electrical and Electronic Engineering, NTU. Since 2008, he has been a Humboldt Research Fellow with the Institute of Microwave Techniques, University of Ulm, Ulm, Germany. His current research interests include the study of multilayer planar circuits, microwave filters and components, planar antennas, numerical modeling and de-embedding techniques, as well as millimeter-wave and microwave antennas for wireless and radar applications.

Dr. Sun was the recipient of a 2008 Hildegard Maier Research Fellowship of the Alexander von Humboldt Foundation, Germany. He was also the recipient of the Young Scientist Travel Grant presented at the 2004 International Symposium on Antennas and Propagation, Sendai, Japan, and the 2002–2005 NTU Research Scholarship, Singapore.